


Polymer Protected and Gel Immobilized Gold and Silver Nanoparticles in Catalysis

Sarkyt E. Kudaibergenov^{1,2}  · Gulnur S. Tatykhanova^{1,2} · Bagadat S. Selenova³

Received: 25 March 2016 / Accepted: 16 April 2016 / Published online: 23 April 2016
© Springer Science+Business Media New York 2016

Abstract This mini-review is focused on preparation of polymer protected gold (AuNPs) and silver (AgNPs) nanoparticles that are immobilized on the surface of inorganic supportors and within hydrogel and/or cryogel matrices. A series of water soluble polymers such as poly(*N*-vinylpyrrolidone), poly(acrylic acid), branched polyethyleneimine, and amphoteric cryogel based on the copolymer of *N,N*-dimethylaminoethylmethacrylate and methacrylic acid poly(DMAEM-MAA) were used for reduction and stabilization of metal nanoparticles. The catalytic properties of polymer protected AuNPs and AgNPs were evaluated with respect to hydrogen peroxide decomposition, hydrogenation of 4-nitrophenol and oxidation of cyclohexane.

Keywords Gold and silver nanoparticles · Water-soluble polymers · Stabilization · Hydrogels · Cryogels · Immobilization · Catalysis · Decomposition · Hydrogenation · Oxidation

Abbreviations

AgNPs Silver nanoparticles
AuNPs Gold nanoparticles

4-AP 4-Aminophenol
BPEI Branched poly(ethyleneimine)
CH Cyclohexane
CH-ol Cyclohexanol
CH-one Cyclohexanone
CuNPs Copper nanoparticles
DLS Dynamic light scattering
DMAEM *N,N*-Dimethylaminoethylmethacrylate
HPEI-IBAM Hyperbranched poly(ethyleneimine) with isobutyramide groups
IL Ionic liquid
kD kiloDalton
MAA Methacrylic acid
MBAA *N,N*-Methylenebisacrylamide
 M_n The number-average molecular weight
4-NA 4-Nitroaniline
NIPAM *N*-Isopropylacrylamide
2-NP 2-Nitrophenol
4-NP 4-Nitrophenol
NPs Nanoparticles
PAA Poly(acrylic acid)
PAAH Poly(acrylamide) hydrogel
PAMAM Poly(amidoamine)
PD1-2 Dendrimer based on poly(ethyleneimine) as a shell and 2,2-bis(palmytyloxymethyl) propionic acid as a dendrone
PdNPs Palladium nanoparticles
PEC Polyelectrolyte complex
PEI Poly(ethyleneimine)

✉ Sarkyt E. Kudaibergenov
skudai@mail.ru

¹ Laboratory of Engineering Profile, K.I. Satpayev Kazakh National Research Technical University, Almaty 050013, Kazakhstan

² Institute of Polymer Materials and Technology, Almaty 050013, Kazakhstan

³ Department of Chemical Technology, K. I. Satpayev Kazakh National Research Technical University, Almaty 050013, Kazakhstan

poly(DMAEM-MAA)	Amphoteric cryogel based on copolymer of <i>N,N</i> -dimethylaminoethylmethacrylate and methacrylic acid
Poly(DMAEM-MAA)/AuNPs	Gold nanoparticles immobilized within poly(DMAEM-MAA) cryogel matrix
PVP	Poly(<i>N</i> -vinylpyrrolidone)
PVP-AgNPs	Silver nanoparticles protected by PVP
PVP-AgNPs/PAAH	Silver nanoparticles protected by PVP and supported onto PAAH
PVP-AgNPs/ZnO	Silver nanoparticles protected by PVP and supported onto ZnO
PVP-AuNPs	Gold nanoparticles protected by PVP
PVP-AuNPs/PAAH	Gold nanoparticles protected by PVP and supported onto PAAH
PVP-AuNPs/ZnO	Gold nanoparticles protected by PVP and supported onto ZnO
SEM	Scanning electron microscope
SOD	Superoxide dismutase
TEM	Transmission electron microscope
TOF	Turnover frequency
TON	Turnover number
UV-Vis	Ultraviolet-Visible spectra

1 Introduction

General principles and recent developments in synthesis, investigation and application of metal nanoparticles have been reviewed in fundamental monographs [1–4]. Among the metal nanoparticles, the AuNPs and AgNPs attracted significant attention due to their unique optical, electrical, biomedical and catalytic properties [5–8]. Hydrophilic polymers possessing nonionic [9–12], anionic [13], cationic [14, 15] and amphoteric [16–18] nature are widely used for reduction and stabilization of AuNPs and AgNPs in solution.

Gold and silver catalysts represent rapidly growing interests due to their potential applicabilities to many reactions of both industrial and environmental importance [19, 20]. Typical examples are the low-temperature catalytic combustion, partial oxidation of hydrocarbons, hydrogenation of carbon oxides and unsaturated hydrocarbons, reduction of nitrogen oxides, and so forth [21]. Recent review [22] describes the size-, shape-, structure- and composition-dependent behavior of AuNPs employed in alkylation, dehydrogenation, hydrogenation, and

selective oxidation reactions for the conversion of hydrocarbons (with main emphasis on fossil resources) to chemicals. The perspectives of substituting platinum group metals for automobile emission control with gold were outlined by authors [23].

Synthesis of gold and silver hydrosols was carried out in one-step process by reduction of aqueous solutions of metal salts using poly(*N*-vinylpyrrolidone) (PVP) [24]. Shape, size, and optical properties of the particles were tuned by changing the employed PVP/metal salt ratio. Size of PVP protected AuNPs ranging from 10 to 110 nm was easily controlled by varying the content of PVP molecules ($0.01\text{--}10\text{ g dL}^{-1}$) [6].

The catalytic activity of AuNPs loaded on the supports (ZnO, Al₂O₃ and MgO) by a colloidal deposition method in benzene conversion was compared [25]. The catalytic activity of AuNPs/ZnO was much greater than that of AuNPs/Al₂O₃ and AuNPs/MgO. The high catalytic activity of the AuNPs/ZnO was attributed to the effects of strong metal-oxide interaction which is possibly originated from the small lattice parameter difference between Au {111} and ZnO {101} lattice planes.

The intrinsic enzyme-like activity of nanoparticles (NPs) has received a great deal of interest due to stability against denaturing, low cost and high resistance to high concentration of substrates compared with natural enzymes. Recent advances in NPs as enzyme mimetics and their analytical and environmental applications were reviewed in [26]. It was demonstrated that AuNPs can act as superoxide dismutase (SOD) and catalase mimetics. Authors [27] reported that AuNPs can catalyze the rapid decomposition of hydrogen peroxide. Molecular recognition of AuNPs and AgNPs together with other noble metal nanoparticles with respect to DNA, proteins, nucleic acids and molecules from the family of supramolecular chemistry was described in review article [28].

The structural combination of a polymer hydrogel network with metal nanoparticles provides superior functionality to the composite materials with potential applications in various fields, including catalysis, electronics, bio-sensing, drug delivery, nano-medicine, and environmental remediation [29, 30]. The review article of Sahiner [31] has been addressed to a flexible and highly adaptable platform for the design of hydrogels with an outlook toward their use in material science, engineering and catalysis. Especially the use of hydrogel matrices for in situ preparation of metal nanoparticles is feasible and readily applicable in the catalysis of various aquatic and non-aquatic reactions.

Cryogels prepared using the cryogelation technique have highly elastic three-dimensional structure consisting of a network of interconnected macropores [32, 33]. Cryogel catalysts could be promising due to the inherent features of these materials: macroporous structures,

adjustable hydrophilicity and hydrophobicity, and flexible choice and combination of catalytic groups. Supporting of noble and transition metal ions in bulk of amphoteric macrogels followed by reduction to zero-valent state will open new perspectives for development of effective catalytic systems for decomposition, isomerization, hydrogenation, and oxidation of various organic substrates [34–36]. In this context design of monolithic support with microporous structure that can provide both nanoparticle loading and liquid flux is challenging task. A considerable effort of researchers is devoted to construct the catalytic system that is highly active, selective, stable, easy to handle, reusable and simple to separate the product from the reaction medium [37]. Superporous cryogels of poly(2-hydroxy ethyl methacrylate) and poly(3-sulfopropyl methacrylate) [38], poly(acrylic acid) [39], poly(4-vinylpyridine) [40], poly(2-acrylamido-2-methyl-1-propanesulfonic acid) [41] and their templated metal nanoparticle composites (Co, Ni, Cu, and Fe) were used in hydrogen generation from the hydrolysis of NaBH_4 and hydrogenation of 4-nitrophenol. Betaine type microgel based on poly(2-(methacryloyloxy) ethyl] dimethyl (3-sulfopropyl) ammonium hydroxide, was used as template for the in situ synthesis of Ni nanoparticles and as catalysts for hydrogenation of nitrogroup containing substrates—4-nitrophenol (4-NP), 2-nitrophenol (2-NP) and 4-nitroaniline (4-NA) [42]. The reduction of substrates is easily monitored by measuring the decrease in the peak of absorption maxima at 414, 400, and 380 nm for 2-, 4-, and 4-NA, respectively.

Our previous literature survey reveals that the number of published papers on the topic of gold catalysis increases substantially [43, 44]. Earlier [45, 46] we have synthesized the PVP protected AuNPs and AgNPs and deposited them on Al_2O_3 by impregnation method. Their catalytic activities were evaluated with respect to hydrogen peroxide decomposition [47]. In the present review we describe the preparation of the AuNPs and AgNPs stabilized by a series of water-soluble and water-swelling polymers possessing nonionic, anionic, cationic and amphoteric character. After characterization of AuNPs and AgNPs in solution and solid state, they were deposited on ZnO supporter, within hydrogel and cryogel matrices and further the catalytic activity of supported catalysts with respect to hydrogen peroxide decomposition, oxidation of cyclohexane, and reduction of 4-nitrophenol was studied.

2 Supporting of Polymer-Protected AuNPs and AgNPs onto ZnO

Scheme 1 illustrates the synthetic pathway of NPs. Boiling of the mixtures of PVP (or poly(acrylic acid) (PAA), branched polyethyleneimine (BPEI), poly(DMAEM-

MAA)), HAuCl_4 and KOH in aqueous solution produces the AuNPs. The water-soluble polymers plays the role of both reducing and stabilizing agents.

The detailed reduction mechanism of HAuCl_4 in presence of PVP was described by authors [48]. The speculative supramolecular interaction between functional groups of PVP and AuNPs with participation of chemisorbed lactame ring is suggested (Scheme 2) [49].

One of the main characteristics of AuNPs and AgNPs is appearance of absorption spectra in visible region due to so-called “plasmon resonance” phenomenon. The colored solutions of AuNPs (PVP-AuNPs) and AgNPs stabilized by PVP (PVP-AgNPs) are shown in Fig. 1. The formation of AuNPs and AgNPs is easily detected due to appearance of the absorption bands at 520–550 and 410–415 nm, respectively (data not given).

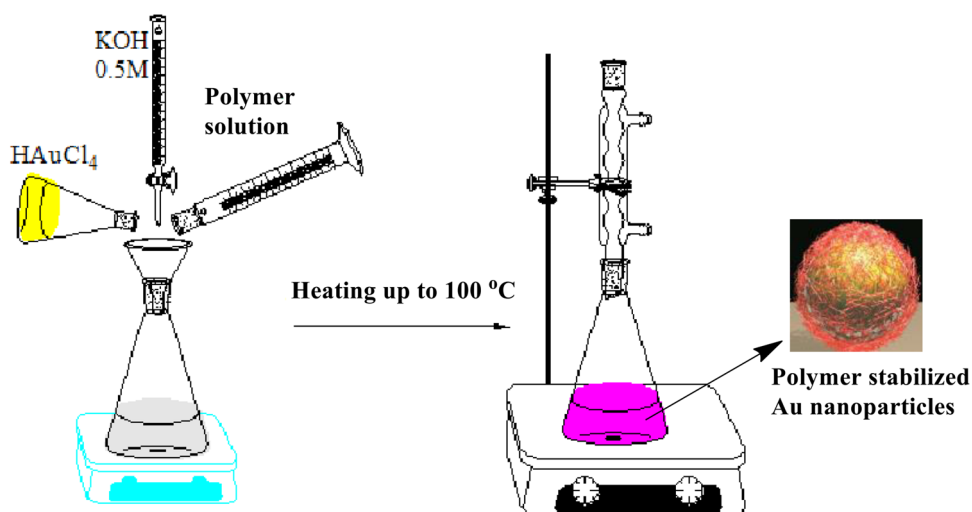
Figures 2 and 3 represent the size distributions of AuNPs and AgNPs stabilized by PVP [49]. In dependence of the number-average molecular weight of PVP (M_n) the average sizes of PVP-AuNPs increase in the following order: PVP-10 kD (~ 10 nm) > PVP-40 kD (~ 15 nm) > PVP-350 kD (~ 25 nm). The average sizes of PVP-AgNPs in dependence of the M_n of PVP increase in the following order: PVP-10 kD (~ 6.5 nm) > PVP-40 kD (~ 12 nm) > PVP-350 kD (~ 44 nm). Thus, the optimal molecular weight of PVP leading to smaller size of AuNPs and AgNPs is PVP-10 kD.

The TEM images clearly show that the average size of the PVP-AuNPs supported on ZnO is 8.2 ± 0.8 nm and smaller than that of PVP-AuNPs in aqueous solution (~ 10 nm) [50]. The PVP-AuNPs images are represented by the small dark particles while ZnO is shown as the larger particles with less intense color (Fig. 4).

3 Immobilization of Polymer-Protected AuNPs and AgNPs Within Hydrogel and Cryogel Matrix

Various synthetic methods have been reported for producing of AuNPs-hydrogel composites: (1) preparation of the nanoparticles and hydrogels separately and then combining the two [51, 52], (2) mixing of the pre-formed nanoparticles with monomer precursor(s) and the polymerization of the mixture [53, 54], (3) embedding of metal salts within hydrogel matrix followed by reduction with the help of reducing agents [55]. The last approach, for instance, was realized for immobilization of AuNPs within NIPAM-based hydrogels [56–58]. As distinct from the abovementioned procedures, the approach of authors [59] is based on “one pot” preparation and immobilization of PEI-protected gold nanoparticles within PAAH in the presence of the ionic liquid (IL)—1-ethyl-3-methylimidazolium ethylsulfate. By

Scheme 1 One-pot synthesis of AuNPs stabilized by water-soluble polymers



Scheme 2 Schematic representation of the supramolecular interaction between PVP and AuNPs

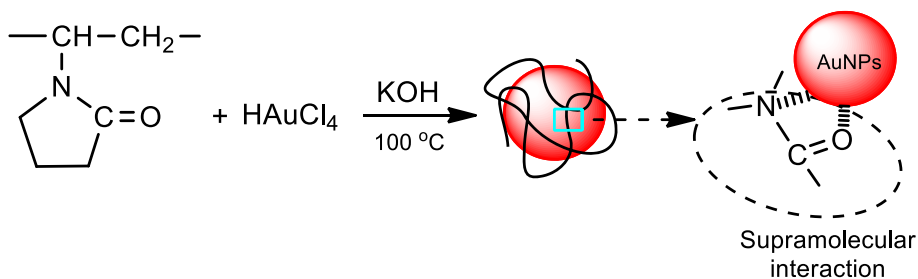


Fig. 1 Samples of AuNPs (1–3) and AgNPs (a–c) stabilized by PVP with $M_n = 10$ kD (1, a), 40 kD (2, b) and 350 kD (3, c)

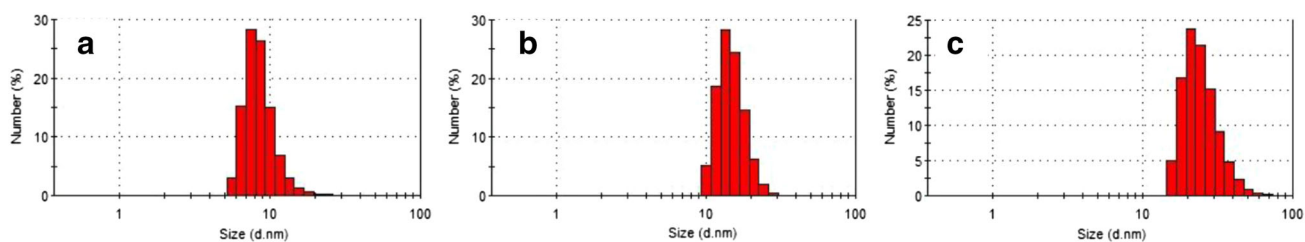
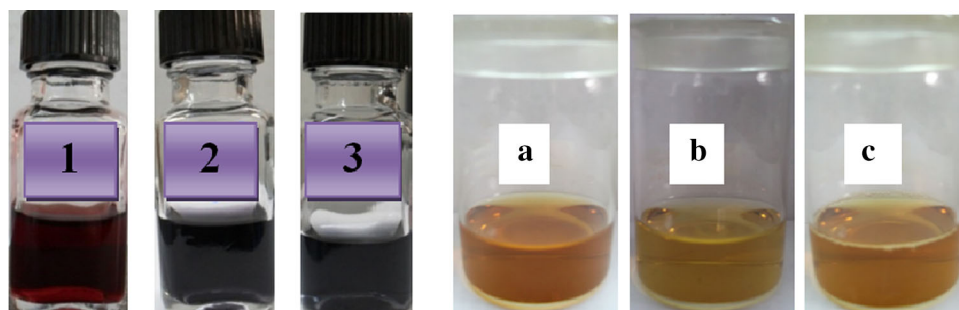


Fig. 2 Size distributions of AuNPs stabilized by PVP with $M_n = 10$ kD (a) 40 kD (b) and 350 kD (c)

regulating the conditions of synthesis and concentration of the components it was possible to change the size and morphology of the formed nanoparticles, as well as to control the gel network parameters.

Hydrogel-immobilized gold nanoparticles were prepared using three approaches: (1) in-situ; (2) adsorption; and (3) borohydride methods [60]. Figure 5 shows the photos and TEM images of PAAH hydrogel samples with

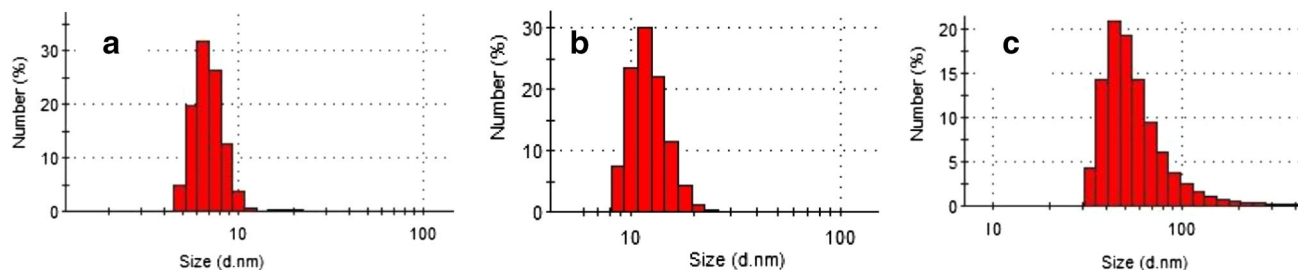


Fig. 3 Size distributions of AgNPs stabilized by PVP with $M_n = 10$ kD (a) 40 kD (b), and 350 kD (c)

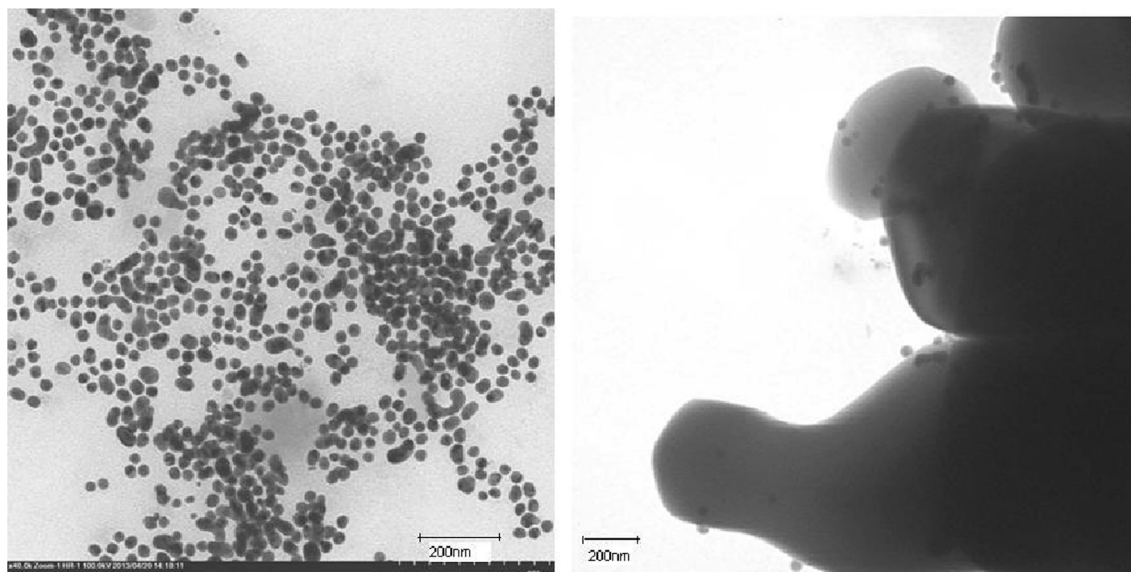


Fig. 4 TEM images of AuNPs protected by PVP-10 kD (left) and deposited onto ZnO (right) [50]

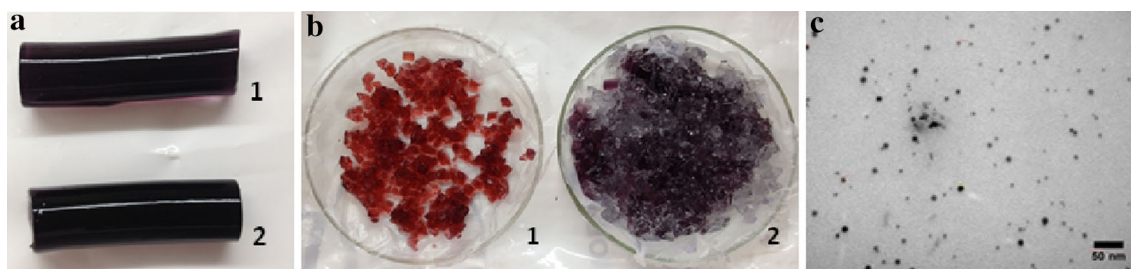


Fig. 5 PVP (1) and BPEI (2) stabilized AuNPs immobilized within PAAH prepared by in-situ (a) and adsorption (b) methods. TEM image of PEI-AuNPs (c) immobilized within PAAH matrix by in-situ method

immobilized AuNPs prepared using in-situ and adsorption methods.

The dimensions of AuNPs in aqueous solution and immobilized within PAAH are compared in Table 1. Analysis of TEM images indicates that in all cases the average size of AuNPs in aqueous solution is considerably smaller than that the average size of AuNPs immobilized

within the PAAH matrix. This may be accounted for aggregation of AuNPs inside of PAAH matrix.

An equimolar amphoteric cryogel poly(DMAEM-MAA) crosslinked by 5 mol% of MBAA was used for immobilization of AuNPs and as catalysts (Fig. 6) [61, 62].

According to SEM images the average pore size of pristine poly(DMAEM-MAA) sample is varied from 40 to

Table 1 The average size of PVP- and PEI-stabilized AuNPs in aqueous solution and in PAAH matrix

Samples	DLS (nm)	TEM (nm)
PVP-AuNPs in aqueous solution	6.5	8.2
PVP-AuNPs/PAAH	Not measurable	46
PEI-AuNPs in aqueous solution	7.0	7.3
PEI-AuNPs/PAAH	Not measurable	128

80 μm (Fig. 7a). The morphology of AuNPs particles on the surface of cryogel is triangular although the hexagonal, spherical and rod-like species are observed (Fig. 7b). The bigger sizes of AuNPs triangles immobilized within poly(DMAEM-MAA) cryogels are varied from 3 to 10 μm .

4 Catalytic Properties of Polymer-Protected and Gel-Immobilized AuNPs and AgNPs

The catalytic properties of AuNPs and AgNPs supported onto zinc oxide, hydrogel and cryogel matrices were evaluated with respect to hydrogen decomposition, 4-nitrophenol hydrogenation and cyclohexane oxidation reactions.

5 Decomposition of Hydrogen Peroxide

5.1 Catalytic Activity of PVP-AuNPs/ZnO in Decomposition of Hydrogen Peroxide

Kinetics and mechanisms of hydrogen peroxide decomposition in presence of metal complexes are well described

in literature [63]. According to ESR spectroscopy measurements [64] the AuNPs generates the reactive oxygen species along with formation of hydroxyl radicals at lower and evolution of O_2 at higher pH.

The influence of catalyst amount (m_{cat}), concentration of substrate ($[\text{H}_2\text{O}_2]$), temperature (T) and molecular weight of PVP (M_n) to find the optimal conditions of H_2O_2 decomposition in presence of PVP-AuNPs/ZnO was studied [49, 50]. It should be mentioned that ZnO itself, without immobilized AuNPs, decomposes only 10 % of H_2O_2 during 4 h. At concentration of $[\text{H}_2\text{O}_2] = 30 \text{ wt}\%$ and $T = 318 \text{ K}$ the decomposition rate of hydrogen peroxide increases with increasing of the m_{cat} (Fig. 8).

As seen from Fig. 6 the rate of decomposition of H_2O_2 at $m_{\text{cat}} = 30 \text{ mg}$ is higher than at $m_{\text{cat}} = 50 \text{ mg}$. Thus the optimal amount of catalyst for H_2O_2 decomposition was accepted as 30 mg. At $m_{\text{cat}} = 30 \text{ mg}$, the decomposition rate of hydrogen peroxide gradually increases with increasing of temperature (Fig. 9). However the rate of H_2O_2 decomposition at $T = 328 \text{ K}$ is close to $T = 318 \text{ K}$, therefore the latter can be considered as optimal temperature.

At $T = 318 \text{ K}$ and $m_{\text{cat}} = 30 \text{ mg}$ the rate of H_2O_2 decomposition increases with increasing of H_2O_2 concentration. However at $[\text{H}_2\text{O}_2] = 40 \text{ wt}\%$ a very fast decomposition of hydrogen peroxide taking places during several minutes is not effective for further oxidation of organic substrates. Therefore it is accepted that the optimal concentration of H_2O_2 is 30 wt%.

Thus the optimal conditions for H_2O_2 decomposition in the presence of PVP-AuNPs/ZnO were equal to: $m_{\text{cat}} = 30 \text{ mg}$, $T = 318 \text{ K}$, $[\text{H}_2\text{O}_2] = 30 \text{ wt}\%$, $M_n = 10 \text{ kD}$. The activation energy of H_2O_2 decomposition is equal to 44.1 kJ mol^{-1} that is lower than the MnO_2 (58 kJ mol^{-1}),

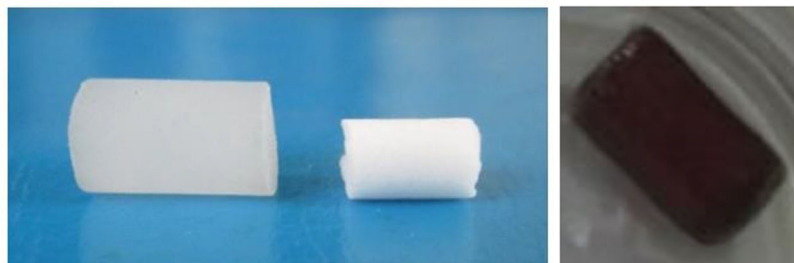
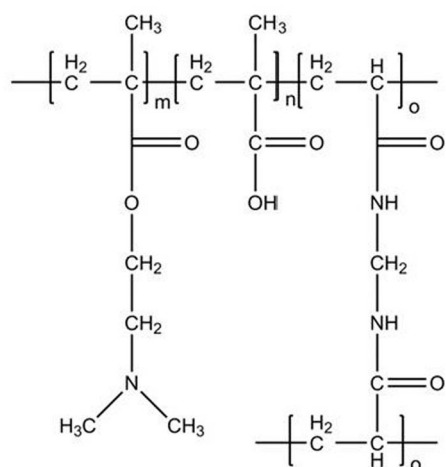


Fig. 6 Structural units of amphoteric cryogels derived from MAA and DMAEM (left), dry, swollen in water and containing the AuNPs cryogel samples (right)

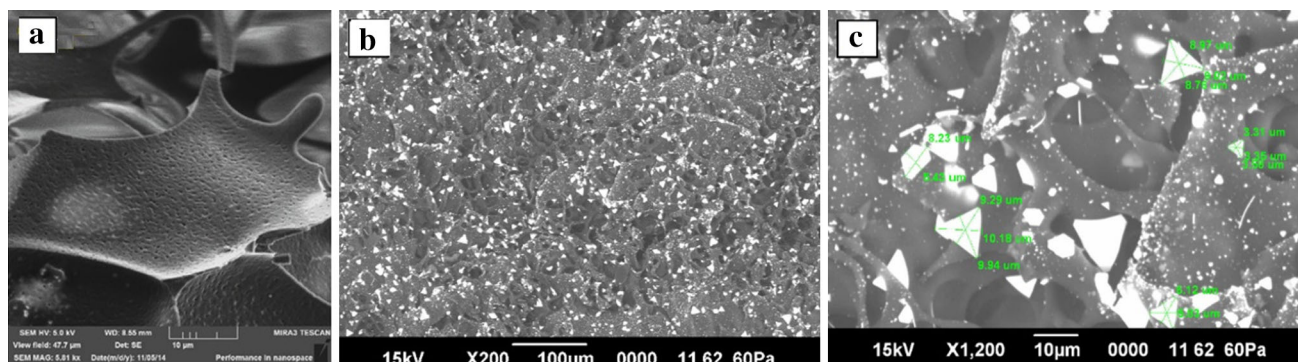


Fig. 7 Morphology of the surface of poly(DMAEM-MAA) (a) and poly(DMAEM-MAA)/AuNPs (b, c)

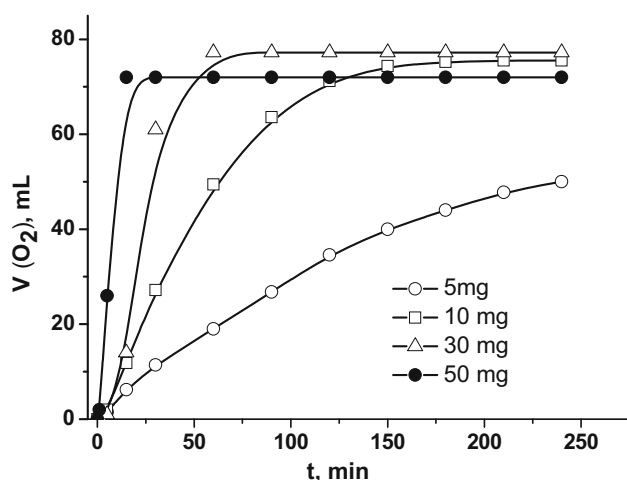


Fig. 8 Decomposition rate of hydrogen peroxide on PVP-AuNPs/ZnO in dependence of the m_{cat} . $T = 318 \text{ K}$, $[\text{H}_2\text{O}_2] = 30 \text{ wt\%}$, $M_n = 10 \text{ kD}$

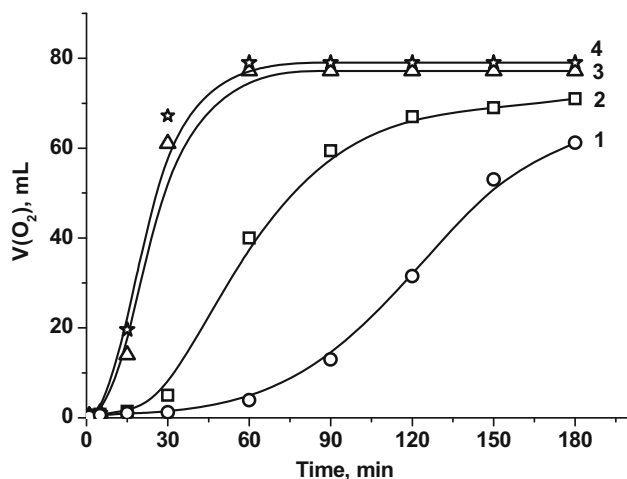


Fig. 9 Decomposition of hydrogen peroxide in the presence of PVP-AuNPs/ZnO at different temperatures. $T = 298$ (1), 308 (2), 318 (3), and 328 K (4). $m_{\text{cat}} = 30 \text{ mg}$, $[\text{H}_2\text{O}_2] = 30 \text{ wt\%}$, $M_n = 10 \text{ kD}$

iodide (56 kJ mol^{-1}) and the platinum metal catalysts (49 kJ mol^{-1}) [65] and higher than iron oxide (32.8 kJ mol^{-1}) [66]. The activation energy of the reaction is about 75 kJ mol^{-1} in the absence of catalyst and is about $7\text{--}8 \text{ kJ mol}^{-1}$ in the presence of catalase [65].

The efficiency of 1 ng of Au to decompose H_2O_2 was also calculated. Since the amount of AuNPs immobilized on the surface of ZnO is not exceeded 0.2 wt%, the content of Au in 30 mg of PVP-AuNPs/ZnO catalyst is about 0.06 mg (or $6 \times 10^4 \text{ ng}$). The maximal amount of released oxygen according to Figs. 8 and 9 is 75–80 mL. Then the ability of 1 ng of Au to produce oxygen is about 1.25–1.50 μL .

The successive decomposition of hydrogen peroxide demonstrates the gradually loss of catalytic activity. In our mind either aggregation or leaching out of AuNPs in the course of hydrogen peroxide decomposition reaction is probably responsible for the observed deactivation during consecutive catalytic runs. Earlier [67] the same phenomenon was observed for PVP protected Pd nanoparticles immobilized within the gel matrix of polyacrylamide after hydrogenation of the successive portions of allyl alcohol.

6 Catalytic Activity of PVP-AgNPs/ZnO in Decomposition of Hydrogen Peroxide

As in case of AuNPs, the AgNPs also generate either hydroxyl radicals at lower pH or oxygen molecules at higher pH [68]. The PVP-AgNPs deposited on ZnO shows a lower catalytic activity than that of PVP-AuNPs [46]. At similar conditions the volume of released oxygen in presence of PVP-AgNPs/ZnO is two times lower than PVP-AuNPs/ZnO. The catalytic activity of PVP-AgNPs/ZnO in dependence of the molecular weight of PVP changes in the next order: PVP(40 kD)-AgNPs/ZnO > PVP(350 kD)-AgNPs/ZnO > PVP(10 kD)-AgNPs/ZnO. Decomposition

of H_2O_2 is too slow and too fast in presence of PVP(10 kD)-AgNPs/ZnO and PVP(40 kD)-AgNPs/ZnO respectively. The optimal molecular weight of PVP seems to be 350 kD. As previously mentioned a very fast decomposition of hydrogen peroxide is not effective for further oxidation of organic substrates.

7 Decomposition of Hydrogen Peroxide by AuNPs Immobilized Within Polyacrylamide Hydrogel (PAAH)

The kinetic curves of hydrogen peroxide decomposition in the presence of gel-immobilized AuNPs prepared using different methods are shown in Figs. 10 and 11 [69].

The catalytic activity of gel-immobilized AuNPs in decomposition reaction of hydrogen peroxide is substantially dependent on the method of their preparation. According to the preparation method the catalytic efficacy is changed as follows: Method 2 (PEI stabilizer) > method 2 (PVP stabilizer) > Method 1 (PEI stabilizer). Thus, the most active catalyst for hydrogen peroxide decomposition is PEI-protected AuNPs immobilized within PAAH and prepared by sorption method 2. In this regard, all further studies for finding optimal decomposition of hydrogen peroxide conditions in the presence of gel-immobilized AuNPs were performed with this catalyst. The optimal conditions decomposition of hydrogen peroxide in the presence of PAAH-immobilized PEI-AuNPs are the following: $T = 318 \text{ K}$, the mass of catalyst is 30 mg, substrate concentration is 30 %.

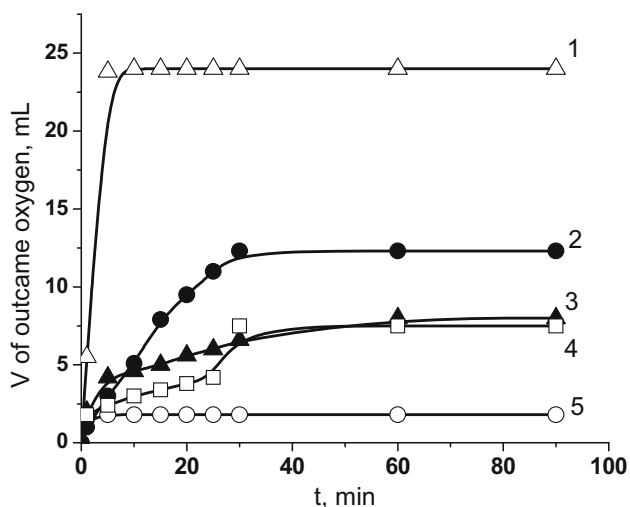


Fig. 10 Decomposition of hydrogen peroxide in presence of PAAH-immobilized AuNPs prepared by sorption method with PEI (1) and PVP (2) as stabilizing agents; borohydrate method (3) and “in-situ” method with PEI (4) and PVP (5) as stabilizing agents. Experimental conditions: $m_{\text{cat}} = 30 \text{ mg}$, $[\text{H}_2\text{O}_2] = 30 \text{ wt\%}$, $T = 318 \text{ K}$

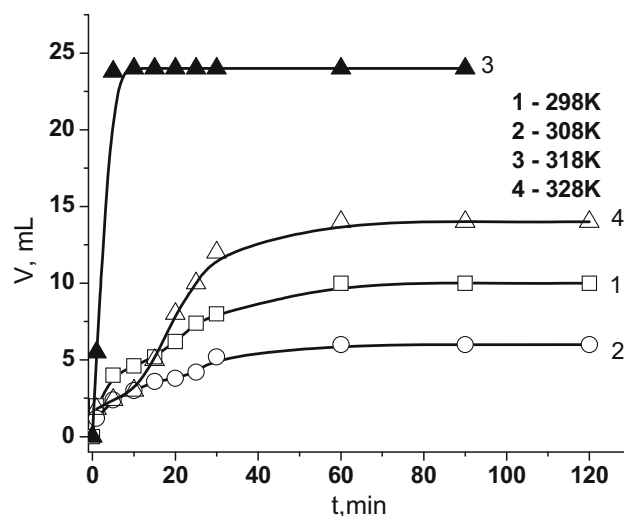


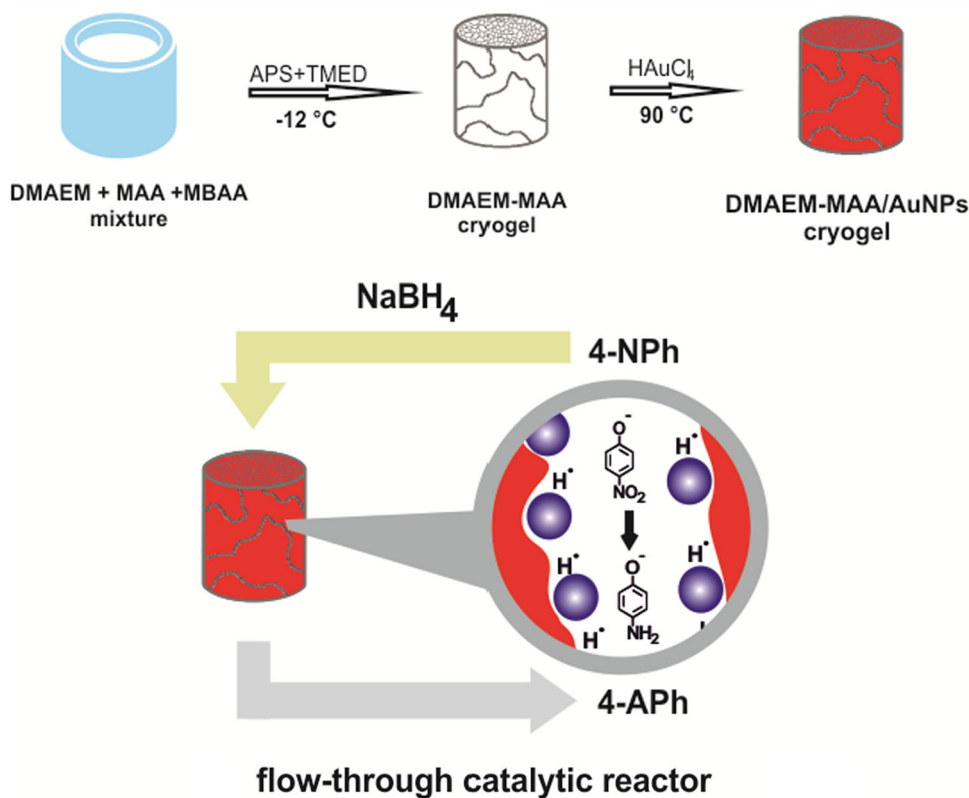
Fig. 11 Temperature dependent decomposition of hydrogen peroxide in the presence of AuNPs-PEI/PAAH prepared by sorption method. $m_{\text{cat}} = 30 \text{ mg}$, $[\text{H}_2\text{O}_2] = 30 \text{ wt\%}$

8 Hydrogenation of 4-Nitrophenol

The reduction of 4-NP to 4-AP by NaBH_4 (or hydrogen) as model reaction is easily monitored by measurement of the absorption spectra of substrate and reaction product at 400 and 300 nm, respectively [70]. In our case the cryogel specimen containing AuNPs served as continuous-flow tank reactor for hydrogenation of 4-NP to 4-AP [62]. The flow-through catalytic reactor represents a glass tube with inner diameter 6–7 mm and height 100 mm which is filled by dry cryogel pieces with diameter 5 mm and height 10 mm. At first 10 or 15 mL of deionized water is passed through the cryogel sample. Due to quick swelling of cryogel the tight sealing between the inner wall of the glass tube and swollen sample takes place. Such simple construction allows the mixture of substrate and reducing agent to flow through the cryogel pores and to create enough contacts between the catalyst and reaction mixture. Passing of the mixture of 4-NP and NaBH_4 through amphoteric cryogel containing AuNPs may cause two effects: the first is additional reduction of Au^{3+} to Au^0 by NaBH_4 , the second is reduction of 4-NP to 4-AP (Fig. 12).

The 95 % conversion is reached during 4 min after five times repeated passing of 10 mL mixture of 4-NP and NaBH_4 through the catalytic reactor (Fig. 13a). The same conversion degree is reached during 13 min after the successive fluxing of 50 mL mixture of 4-NP and NaBH_4 (Fig. 13b). The poly(DMAEM-MAA)/AuNPs preserved the high catalytic activity even after passing of 100 mL of 4-NP and NaBH_4 mixture. In our mind 100 % conversion of 4-NP is not reachable due to capturing of some amounts of substrate in dead volume of cryogel. It should be noted

Fig. 12 Schematic representation of flow-through catalytic reactor



that neither the mixture of 4-NP and NaBH_4 itself, nor the mixture of 4-NP and NaBH_4 fluxed through the poly (DMAEM-MAA) cryogel does not produce 4-AP in absence of immobilized AuNPs.

The reduction rate constant of 4-NP has the pseudo-first-order and depends on the concentration of nitrophenolate-anion rather than concentration of NaBH_4 due to its excess

[71]. The kinetics of 4-NP reduction is expressed by equation

$$\ln\left(\frac{c_t}{c_o}\right) = \ln\left(\frac{D_t}{D_o}\right) = -k * t \quad (1)$$

where C_t and C_0 are concentrations, D_t and D_0 are optical densities of nitrophenolate-anions at definite time t and $t = 0$.

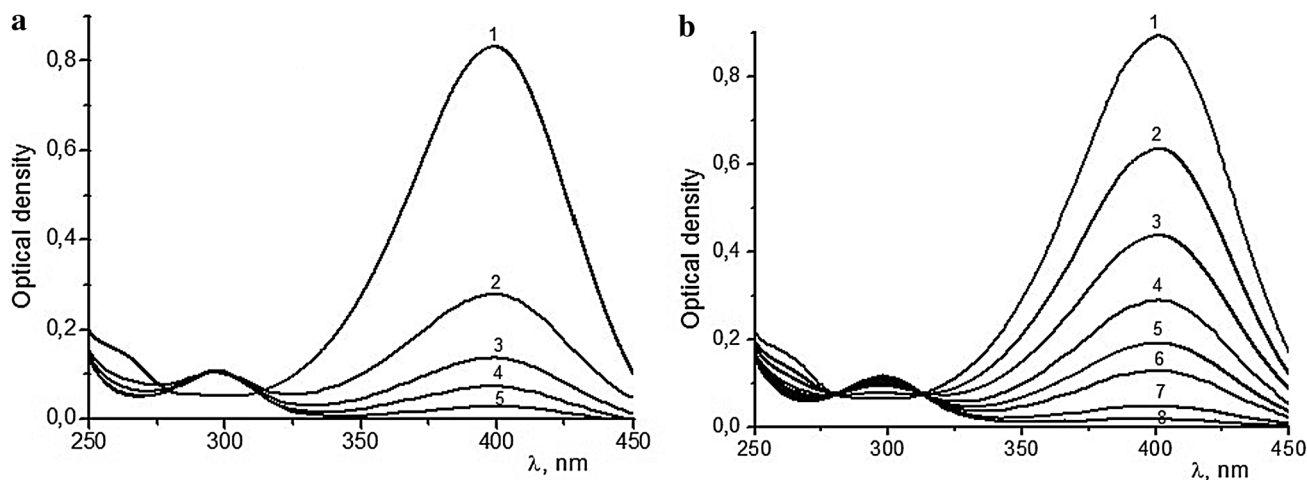


Fig. 13 The time dependent absorbance spectra of 4-NP and 4-AP during the 1st (a) and 5th (b) process cyclicality. $t = 0$ (curve 1), 1 (curve 2), 2 (curve 3), 3 (curve 4), 4 (curve 5), 5 (curve 6), 8 (curve 7), 11 (curve 8) min

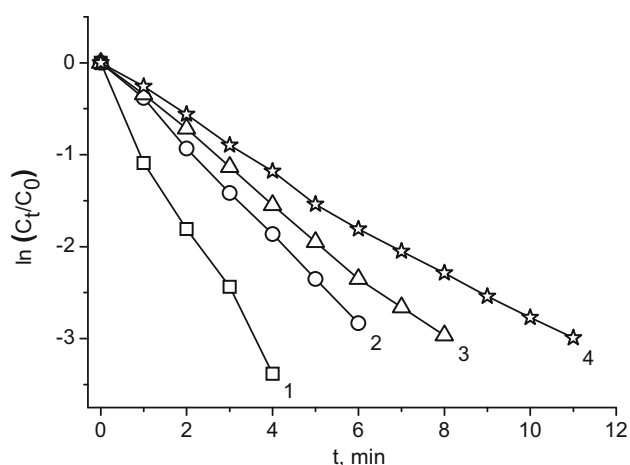


Fig. 14 The reaction kinetic curves of $\ln(C_t/C_0)$ versus time as a function of process cyclicality. The 1st cycle (1), the 2nd cycle (2), the 5th cycle (3), the 10th cycle (4)

The logarithmic dependence of the Eq. (1) has linear character and shows that the first cycle is completed during 4 min with 95 % conversion, the second cycle—after 6 min, while the 95 % conversion of 4-NP to 4-AP during 10 cycles requires 11 min (Fig. 14). The apparent rate constants (k_{app}) found from the slopes of kinetic curves of Fig. 14 during the 1st, 2nd, 5th, and 10th reduction cycles of 4-NP are equal to $13.5 \times 10^{-3} \text{ s}^{-1}$, $8 \times 10^{-3} \text{ s}^{-1}$, $6.3 \times 10^{-3} \text{ s}^{-1}$, and $4.6 \times 10^{-3} \text{ s}^{-1}$. Thus, the k_{app} value decreases with increasing of process cyclicality. Cryogel catalyst sustained over 10 cycles without loss of activity.

The kinetic rate constant of poly(DMAEM-MAA)/AuNPs for the reduction of 4-NP to 4-AP was compared with literature data (Table 2).

Comparative analysis shows that poly(DMAEM-MAA)/AuNPs catalyst occupies intermediate position among the catalytic systems used for reduction of 4- to 4-AP. The detailed mechanism of the reduction of 4-NP on the surface of AuNPs is given by authors [79]. In our mind the 4-NP molecules are stabilized within the inner surface of poly(DMAEM-MAA)/AuNPs via hydrogen bonds between OH groups of substrate and COOH (or $-\text{N}(\text{CH}_3)_2$) groups of cryogel. The immobilized AuNPs in cryogel pores generates hydrogen atoms from the NaBH_4 that in its turn hydrogenate the nitro groups. Detachment of 4-AP molecules from the surface of poly(DMAEM-MAA)/AuNPs takes place due to electrostatic repulsion, e.g. the negatively charged surface of AuNPs repels the same charged 4-nitrophenolate anions from the reaction mixture. The lifetime of the catalyst is usually expressed through the turnover number (TON) that is the number of moles of substrate that a mole of the catalyst can convert before inactivation [80]. The stability of poly(DMAEM-MAA)/AuNPs catalyst, the so-called TON that is defined as

$$TON = \frac{[4 - \text{NP}]}{[\text{AuNPs}]} \times OCT \quad (2)$$

(where $[4\text{-NP}]$ and $[\text{AuNPs}]$ are the molar concentrations of substrate and catalyst, OCT is the overall catalytic time) and the turnover frequency (TOF) calculated (for the first cycle) according to equation

$$TON = \frac{[4 - \text{NP}] \cdot [\text{conversion}]}{[\text{AuNPs}] \cdot t} \quad (3)$$

was equal to $TON = 38.17$ and $TOF = 21.56 \text{ h}^{-1}$, respectively.

Table 2 The rate constants of the reduction of 4-NP to 4-AP catalyzed by metal nanoparticles supported on various polymers

Type of catalyst	Rate constant, $\times 10^{-2} \text{ s}^{-1}$	Ref.
PEI/AuNPs	4.6	[71]
PEI- C_{12} /AuNPs	5.2	[71]
HPEI-IBAM/AuNPs	$\approx 2\text{--}3$	[70]
Chitosan/AuNPs	0.24	[72]
Resin/AuNPs	2.5	[73]
Chitosan/FeNPs	0.24	[74]
PEC/AuNPs	0.5	
PEC/PdNPs	0.394	
PEC/AgNPs	0.142	[75]
PEC/AuNPs ₅₀ /AgNPs ₅₀	0.678	
PEC/AuNPs ₅₀ /AgNPs ₂₅ /PdNPs ₂₅	0.983	
PAMAM dendrimers/AuNPs	2.51	[76]
PAMAM dendrimers/AgNPs	0.71	
PAMAM dendrimers/CuNPs	2.43	
PD1-2/AuNPs	≈ 2.8	[77]
Poly(DMAEM-MAA)/AuNPs	1.35	[62, 78]

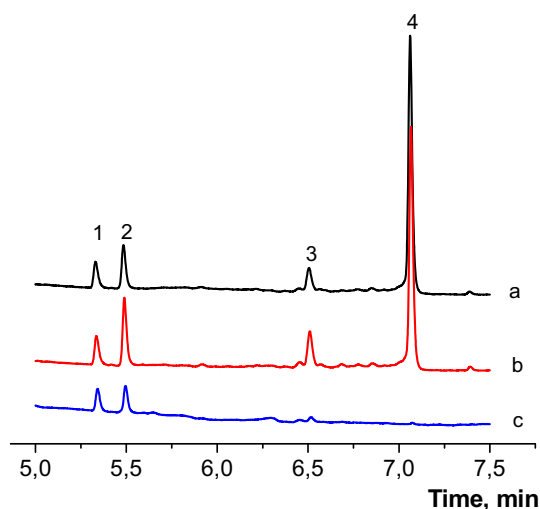


Fig. 15 Chromatograms of the products of cyclohexane oxidation catalyzed by BPEI-AuNPs/ZnO (a), PAA-AuNPs/ZnO (b) and PVP-AuNPs/ZnO (c). Product identification: 1—CH-ol, 2—CH-one, 3—aldehydes, 4—carboxylic acids. Oxidation conditions: $m_{\text{cat}} = 70$ mg, solvent—acetonitrile is 4 mL, $V_{\text{CH}} = 1$ mL, $[\text{H}_2\text{O}_2] = 30\%$, $V_{\text{H}_2\text{O}_2} = 0.6$ mL, $T = 348$ K, $t = 6$ h

9 Oxidation of Cyclohexane (CH)

The oxidation of CH is of greatest interest because the reaction products of cyclohexane—cyclohexanol (CH-ol) and cyclohexanone (CH-one) are the key products for the production of adipic acid that is further used itself in the food industry and as lubricant materials as well as for preparation of polyamide materials, plastics, and foams [81]. In industrial conditions the oxidation of CH to CH-one and CH-ol proceeds in the presence of homogeneous or heterogeneous catalysts at the interval of temperature 140–160 °C and pressure 1 atm. The selectivity of the oxidation process is 60–70 %, conversion reaches up to 10 % [82].

Figure 15 shows the chromatograms of the oxidation products of CH by PVP-AuNPs/ZnO, PAA-AuNPs/ZnO, and BPEI-AuNPs/ZnO [60]. The catalyst based on PVP-AuNPs/ZnO mostly converts the CH to CH-ol and CH-one while in the presence of PAA-AuNPs/ZnO and BPEI-

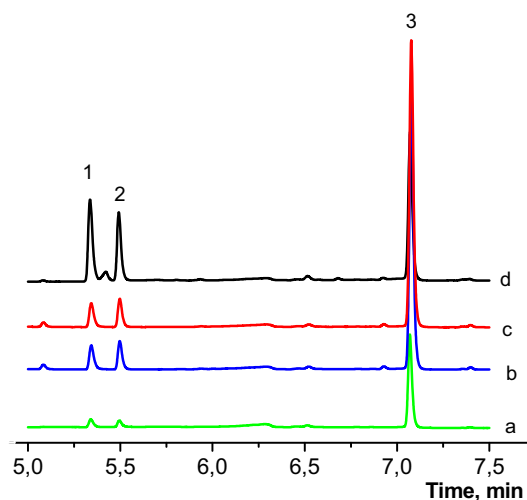


Fig. 16 Chromatograms of the products of cyclohexane oxidation catalyzed by PEI-AuNPs/PAAH (in situ method) (a), PVP-AuNPs/PAAH (adsorption method) (b), AuNPs/PAAH (borohydride method) (c), BPEI-AuNPs/PAAH (adsorption method) (d). Oxidation conditions: $m_{\text{cat}} = 30$ mg, $V_{\text{CH}} = 1$ mL, $[\text{H}_2\text{O}_2] = 30\%$, $V_{\text{H}_2\text{O}_2} = 0.6$ mL, $T = 318$ K, $t = 6$ h

AuNPs/ZnO the main oxidation products of CH are both aldehydes and carboxylic acids (Table 3). However the conversion of CH in all cases is too low (1.0–3.4 %).

According to chromatographic analysis (Fig. 16), the yield of CH-ol, CH-one and carboxylic acids in the presence of BPEI-AuNPs/PAAH (prepared by adsorption method) is 29.5, 22.5 and 48 %, respectively; the conversion is 37 % (Table 4). In the presence of BPEI-AuNPs/PAAH (prepared by “in-situ” method), PVP-AuNPs/PAAH (prepared by adsorption method), and AuNPs/PAAH (prepared by borohydride method) the conversion is low and varies between 5 and 7 %, the yield of CH-ol is in the range of 7.6–8.7 %, the yield of CH-one is 6.5–8.4 %, the yield of carboxylic acids is 83.8–85.6 %. In spite of high yield of carboxylic acids, the conversion of the CH is low and varies between 5.1 and 7.2 %. Thus, the best catalyst for the oxidation of CH to CH-ol and CH-one is AuNPs stabilized with BPEI and immobilized into the matrix of PAAH and prepared by adsorption method.

Table 3 The results of chromatographic analysis of the oxidation products of CH catalyzed by PVP-AuNPs/ZnO, PAA-AuNPs/ZnO, BPEI-AuNPs/ZnO

Catalyst	CH-ol (%)	CH-one (%)	Aldehydes (%)	Carboxylic acids (%)	Conversion (%)
PVP-AuNPs/ZnO	43.00	55.00	Trace	Trace	1.00
PAA-AuNPs/ZnO	8.80	18.70	10.12	62.37	3.00
BPEI-AuNPs/ZnO	8.45	13.00	6.40	72.20	3.40

Table 4 The results of chromatographic analysis of the oxidation products of CH catalyzed by PVP-AuNPs/PAAH and BPEI-AuNPs/PAAH

Catalyst	CH-ol (%)	CH-one (%)	Aldehydes (%)	Carboxylic acids (%)	Conversion (%)
BPEI-AuNPs/PAAH adsorption method	29.5	22.5	Trace	48.0	37
BPEI-AuNPs/PAAH in situ method	7.9	6.5	Trace	85.6	7.2
PVP-AuNPs/PAAH adsorption method	7.6	8.4	Trace	84.0	6.4
AuNPs/PAAH borohydride method	8.7	7.5	Trace	83.8	5.1

While the catalysts BPEI-AuNPs/PAAH (prepared by “in-situ” method), PVP-AuNPs/PAAH (prepared by adsorption method), and AuNPs/PAAH (prepared by borohydride method) are more selective with respect to carboxylic acids.

Thus the oxidation products of CH in the presence of AuNPs protected by water-soluble polymers and immobilized on ZnO and PAAH supporters are CH-ol, CH-one, aldehydes and carboxylic acids with various yields and conversions. The further experiments should be carried out to increase the selectivity of catalysts with respect to desired key products and to find the optimal conditions of catalytic reactions.

10 Conclusion

Gold (AuNPs) and silver (AgNPs) nanoparticles were prepared by “one-pot” synthetic protocol, e.g. by boiling of the aqueous solution of HAuCl₄ and KOH in the presence of various water-soluble polymers. The DLS, SEM and TEM results reveal that the average size of AuNPs and AgNPs stabilized by PVP is varied from 10 to 25 nm and from 6.5 to 44 nm, respectively. It was established that the average sizes of AuNPs and AgNPs stabilized by PVP in aqueous solution increase with increasing of the molecular weight of PVP. The TEM images indicate that the average size of AuNPs in aqueous solution is considerably smaller than that the average size of AuNPs immobilized within the PAAH matrix. This may be accounted for aggregation of AuNPs inside of PAAH matrix. Polymer-protected gold and silver nanoparticles supported on zinc oxide were used as nanosized catalysts in decomposition of hydrogen peroxide. The optimal conditions H₂O₂ decomposition in dependence of catalysts amount, concentration of substrate, molecular weight of PVP, and temperature were found. The catalytic properties of AuNPs immobilized within PAAH matrix were evaluated. The catalytic activity of gel-immobilized AuNPs in decomposition of hydrogen peroxide is substantially dependent on the method of their preparation. According to the preparation procedure, the most active catalyst for hydrogen peroxide decomposition is BPEI-protected AuNPs immobilized within PAAH and

prepared by adsorption method. It was found that the most effective catalysts for oxidation of CH to CH-ol and CH-one are PVP-AuNPs/ZnO and BPEI-AuNPs/PAAH (prepared by adsorption method). The rest catalysts are more selective for conversion of CH to carboxylic acids. Amphoteric cryogel based on poly(DMAEM-MAA) was synthesized by cryopolymerization technique. SEM images of cryogel show sponge-like porous structure composed of interconnected channels. The AuNPs are mostly accumulated on the surface of cryogel in the form of spherical and triangular AuNPs species of different sizes. Passing of the mixture of 4-NP and NaBH₄ through amphoteric cryogel containing AuNPs leads to additional reduction of Au³⁺ to Au⁰ and reduction of 4-NP to 4-AP. The turnover number (TON) and the turnover frequency (TOF) of cryogel catalyst are equal to 38.17 and 21.56 h⁻¹, respectively. The potential application of amphoteric cryogel samples with immobilized AuNPs as effective flow-through units for continuous hydrogenation of 4-NP is demonstrated.

Acknowledgments Financial support from the Ministry of Education and Science of the Republic of Kazakhstan in the frame of the Grant No. 1004/GF4 2015–2017 is greatly acknowledged.

References

1. A.D. Pomogailo, G.I. Dzhardimalieva, *Metallopolymeric Hybrid Nanocomposites* (Nauka, Moscow, 2015)
2. A.D. Pomogailo, A.S. Rozenberg, I.E. Uflyand, *Metal Nanoparticles in Polymers* (Khimiya, Moscow, 2000)
3. E.A. Bekturov, S.E. Kudaibergenov, R.M. Iskakov, A.K. Zhar-magambetova, Zh.E. Ibraeva, S. Shmakov, *Polymer-Protected Nanoparticles of Metals*, Almaty (2010). **In Russian**
4. Zh.E. Ibrayeva, S.E. Kudaibergenov, E.A. Bekturov, *Stabilization of metal nanoparticles by hydrophilic polymers* (Lambert Academic Publishing, Saarbrücken, 2013). **In Russian**
5. J. Shan, H. Tenhu, *Chem. Commun.* **44**, 4580 (2007)
6. P. Zhao, N. Li, D. Astruc, *Coord. Chem. Rev.* **257**, 638 (2013)
7. J. Zhou, J. Ralston, R. Sedev, D.A. Beattie, *J. Colloid Interface Sci.* **331**, 251 (2009)
8. S.K. Balasubramanian, L. Yang, L.-Y.L. Yung, Ch-N Ong, W.-Y. Ong, L.E. Yu, *Biomaterials* **31**, 9023 (2010)
9. S. Ram, L. Agrawal, A. Mishra, S.K. Roy, *Adv. Sci. Lett.* **4**, 3431 (2011)
10. J.W. Chung, Y. Guo, S.-Y. Kwak, R.D. Priestley, *J. Mater. Chem.* **22**, 6017 (2012)

11. B.J. Morrow, E. Matijević, D.V. Goia, *J. Colloid Interface Sci.* **335**, 62 (2009)
12. A. Dorris, S. Rucareanu, L. Reven, C.J. Barrett, L.R. Bruce, *Langmuir* **24**, 2532 (2008)
13. R. Sardar, N.S. Bjorge, J.S. Shumaker-Parry, *Macromolecules* **41**, 4347 (2008)
14. H. Chen, D.M. Lentz, R.C. Hedden, *J. Nanopart. Res.* **14**, 682 (2012)
15. C. Note, J. Koetz, L. Wattebled, A. Laschewsky, *J. Colloid Interface Sci.* **308**, 162 (2007)
16. S. Li, Y. Wu, J. Wang, Q. Zhang, Y. Kou, Zhang S. *J. Mater. Chem.* **20**, 4379 (2010)
17. B. Mahltig, N. Cheval, J.-F. Gohy, A. Fahmi, *J. Polym. Res.* **17**, 579 (2010)
18. P. Zhao, N. Li, D. Astruc, *Coord. Chem. Rev.* **257**, 638 (2013)
19. M. Haruta, *Catal. Surv. Jpn.* **1**, 61 (1997)
20. Zh.-J. Jiang, Ch.-Y. Lui, L.-W. Sun, *J. Phys. Chem. B.* **109**, 1730 (2005)
21. M. Haruta, M. Daté, *Appl. Catal. A* **222**, 427 (2001)
22. N.R. Shiju, V.V. Gulians, *Appl. Catal. A* **356**, 1 (2009)
23. Y. Zhang, R.W. Catrall, I.D. McKelvie, S.D. Kolev, *Gold Bull.* **44**, 145 (2011)
24. C.E. Hoppe, M. Lazzari, I. Pardinias-Blanco, M.A. Lopez-Quintela, *Langmuir* **22**, 7027 (2006)
25. H. Wu, L. Wang, J. Zhang, Z. Shen, J. Zhao, *Catal. Commun.* **12**, 859 (2011)
26. J. Xie, X. Zhang, H. Wang, H. Zheng, Y. Huang, *Trends Anal. Chem.* **39**, 114 (2012)
27. W. He, Y.-T. Zhou, W.G. Wamer, X. Hu, X. Wu, Z. Zheng et al., *Biomaterials* **34**, 765 (2013)
28. Y. Tauran, A. Brioude, A.W. Coleman, M. Rhimi, B. Kim, *World J. Biol. Chem.* **4**, 35 (2013)
29. E.M. Ahmed, *J. Adv. Res.* **6**, 105 (2015)
30. P. Thoniyot, M.J. Tan, A.A. Karim, D.J. Young, X. Jun, Loh, *Adv. Sci.* (2015). doi:10.1002/advs.201400010
31. N. Sahiner, *Prog. Polym. Sci.* **38**, 1329 (2013)
32. V.I. Lozinsky, *Russ. Chem. Rev.* **71**, 489 (2002)
33. B. Mattiasson, A. Kumar, I. Galaev, *Macroporous polymers: production properties and biotechnological/biomedical applications* (CRC, Boca Raton, 2010)
34. S.E. Kudaibergenov, N. Nuraje, V.V. Khutoryanskiy, *Soft Matter* **8**, 9302 (2012)
35. G. Tatykhanova, Zh. Sadakbayeva, D. Berillo, I. Galaev, Kh. Abdullin, Zh. Adilov, S. Kudaibergenov, *Macromol. Symp.* **7**, 317 (2012)
36. S. Kudaibergenov, Z. Adilov, D. Berillo, G. Tatykhanova, Z. Sadakbaeva, K. Abdullin, I. Galaev, *eXPRESS Polym. Lett.* **6**, 346 (2012)
37. H. Koga, T. Kitaoka, *Chem. Eng. J.* **68**, 420 (2011)
38. N. Sahiner, S. Yildiz, M. Sahiner, *Appl. Surf. Sci.* **354**, 388 (2015)
39. N. Sahiner, F. Seven, *Energy* **71**, 170 (2014)
40. N. Sahiner, S. Yildiz, *Fuel Process. Technol.* **126**, 324 (2014)
41. N. Sahiner, F. Seven, *RSC Adv.* **4**, 23886 (2014)
42. M. Ajmal, S. Demirci, M. Siddiq, N. Aktas, N. Sahiner, *Colloids Surf. A* **486**, 29 (2015)
43. E.K. Baygazieva, N.N. Yesmurzayeva, G.S. Tatykhanova, G.A. Mun, V.V. Khutoryanskiy, S.E. Kudaibergenov, *Int. J. Biol. Chem.* **7**, 14 (2014)
44. S.E. Kudaibergenov, G.S. Tatykhanova, *Int. J. Biol. Chem.* **6**, 40 (2013)
45. S.E. Kudaibergenov, G.S. Tatykhanova, E.K. Baigazyeva, *Proceedings of the International Conference Nanomaterials: Applications and Properties*, Sumy State University, vol 1(1), p. 01PCN42, 3 (2012)
46. S.E. Kudaibergenov, E.K. Baigazyeva, N.N. Yesmurzayeva, Z.A. Nurakhmetova, B.S. Selenova, *Proceedings of the International Conference Nanomaterials: Applications and Properties*, Sumy State University, vol 2(1), p. 02PCN03, 4 (2013)
47. N. Yesmurzayeva, B. Selenova, S. Kudaibergenov, *J. Am. Nanomater.* **1**, 1 (2013)
48. C.E. Hoppe, M. Lazzari, I. Pardinias-Blanco, M.A. Lopez-Quintela, *Langmuir* **22**, 7027 (2006)
49. N.N. Yesmurzayeva, B.S. Selenova, S.E. Kudaibergenov, *Supramol. Catal.* **2**, 1 (2015)
50. Zh. Ibrayeva, E. Baigazyeva, N. Yesmurzayeva, G. Tatykhanova, M. Yashkarova, S. Kudaibergenov, *Macromol. Symp.* **351**, 51 (2015)
51. V. Pardo-Yissar, R. Gabai, A.N. Shipway, T. Bourenko, I. Willner, *Adv. Mater.* **13**, 1320 (2001)
52. L. Sheeney-Hai-ichia, G. Sharabi, I. Willner, *Adv. Funct. Mater.* **12**, 27 (2002)
53. J.M. Weissman, H.B. Sunkara, A.S. Tse, S.A. Asher, *Science* **274**, 959 (1996)
54. J.H. Holtz, S.A. Asher, *Nature* **389**, 829 (1997)
55. Y.-J. Lee, P.V. Braun, *Adv. Mater.* **15**, 563 (2003)
56. C. Echeverria, C. Mijangos, *Macromol. Rapid Commun.* **31**, 54 (2010)
57. C. Wang, N.T. Flynn, R. Langer, *Mater. Res. Soc. Symp. Proc.* **820**, R.1.2.1 (2004)
58. J. Zhang, B. Zhao, L. Meng, H. Wu, X. Wang, Ch. Li, J. Nanopart. Res. **9**, 1167 (2007)
59. N. Dolya, O. Rojas, S. Kosmella, B. Tiersch, J. Koetz, S. Kudaibergenov, *Macromol. Chem. Phys.* (2013). doi:10.1002/macp.201200727
60. E.K. Nurgazyeva, G.S. Tatykhanova, G.A. Mun, V.V. Khutoryanskiy, S.E. Kudaibergenov, *Int. J. Biol. Chem.* **8**, 61 (2015)
61. A.N. Klivenko, A. Bolat, S.E. Kudaibergenov, G.A. Mun, *Bull. Nat. Eng. Acad. RK.* **3**, 85 (2014)
62. A.N. Klivenko, G.S. Tatykhanova, N. Nuraje, S.E. Kudaibergenov, *Chem. Bull. Karaganda State Univ.* **4**, 10 (2015)
63. A.I.A. Saleem, M. El-Maazawi, A.B. Zaki, *Int. J. Chem. Kinet.* **32**, 643 (2000)
64. W. He, Y.-T. Zhou, W.G. Wamer, X. Hu, X. Wu, Z. Zheng et al., *Biomaterials* **34**, 765 (2013)
65. E.A. Moelwyn-Hughes, *Physical Chemistry* (Pergamon, London, 1957)
66. S.-S. Li, M.D. Gurol, *Environ. Sci. Technol.* **32**, 1417 (1998)
67. S. Kudaibergenov, Zh. Ibraeva, N. Dolya, B. Musabayeva, K. Zharmagambetova, J. Koetz, *Macromol. Symp.* **274**, 11 (2006)
68. W. He, Y.-T. Zhou, W.G. Wamer, M.D. Boudreau, J.-J. Yin, *Biomaterials* **33**, 7547 (2012)
69. E. Nurgazyeva, G. Tatykhanova, G. Mun, V. Khutoryanskiy, S. Kudaibergenov, *Proceedings of the International Conference Nanomaterials: Applications and Properties*, Sumy State University, vol 4, p. 02NNSA11, 4 (2015)
70. X.-Y. Liu, F. Cheng, Y. Liu, H.J. Liu, Y.J. Chen, *Mater. Chem.* **20**, 360 (2010)
71. P. Veerakumar, M. Velayudham, K.-L. Lu, S. Rajagopal, *Appl. Catal. A* **439**, 197 (2012)
72. R. Seoudi, D.A. Said, *World J. Nanosci. Eng.* **1**, 51 (2011)
73. D. Shah, H. Kaur, *J. Mol. Catal. A* **381**, 70 (2014)
74. H. Lu, Q.X. Xueliang, W. Wang, F. Tan, Z. Xiao, J. Chen, *Micro NanoLett.* **9**, 446 (2014)
75. M.S. Islam, W.S. Choi, H.-J. Lee, *Int. J. Mater. Mech. Manuf.* **2**, 1 (2014)
76. M. Nemanashi, R. Meijboom, *J. Colloid Interface Sci.* **389**, 260 (2013)

77. Y. Liu, Y. Fan, Y. Yuan, Y. Chen, F. Cheng, J. Shi-Chun, J. Mater. Chem. **22**, 21173 (2012)
78. G.S. Tatykhanova, A.N. Klivenko, G.M. Kudaibergenova, S.E. Kudaibergenov. Macromol. Symp. (to be published) (2016)
79. P. Veerakumar, M. Velayudham, K.-L. Lu, S. Rajagopal, Appl. Catal. **439**, 197 (2012)
80. S. Creutz, P. Teyssie, R. Jerome, Macromolecules **30**, 6 (1997)
81. I.V. Berezin, E.T. Denisov, N.M. Emanuel, *Oxidation of Cyclohexane* (Moscow State University, Moscow, 1962)
82. L.A. Vakhovskaya, S.V. Kruglov, B.G. Freidin, J. Appl. Chem. **51**, 1345 (1978)